Article

Journal of
Nanoscience and Nanotechnology
Vol. 18, 1–8, 2018
www.aspbs.com/jnn

Effect of O_2 Concentration on the Electrochromic Properties of NiO_x Films

Jianhua Qiu[1, 2, *], Zhao Chen[1], Tianxiang Zhao[1], Zhihui Chen[1], Wenjing Chu[3], Ningyi Yuan[1], and Jianning Ding[1, 2]

[1] *School of Mathematics and Physics, Jiangsu Province Cultivation Base for State Key Laboratory of Photovoltaic Science and Technology, Jiangsu Collaborative Innovation Center of Photovolatic Science and Engineering, Changzhou University, Changzhou 213164, Jiangsu, China*
[2] *School of Mechanical Engineering, Jiangsu University, Zhenjiang, 212013, Jiangsu, China*
[3] *Provincial Photoelectric Glass Key Laboratory, Changzhou Almaden Co., Ltd., Changzhou 213000, Jiangsu, China*

Nickel oxide (NiO_x) films were deposited onto ITO-coated glass at room temperature by DC magnetron sputtering in Ar/O_2 mixing gas. The effect of O_2 concentration on structure, morphology, electrochemical and electrochromic properties of NiO_x films was systematically investigated. X-ray diffraction results showed NiO_x films had the polycrystalline structure. NiO_x films deposited at low O_2 concentration had the preferred (200) peak. On the other hand, the films exhibited the strong (111) peak at high O_2 concentration. Small roughness and grain size of NiO_x film deposited at 15% O_2 concentration were observed by atomic force microscope and scanning electron microscope results, and small crystallite size was obtained from the XRD data which leads to the good cyclic durability. The large transmittance modulation, high color efficiency and fast coloring/bleaching response time make NiO_x films suitable to be applied as an anodic coloring material complemented with WO_3 electrochromic window.

Keywords: Magnetron Sputtering, Nickel Oxide, Electrochromism, Transmittance Modulation.

1. INTRODUCTION

Electrochromic devices, exhibited a reversible change of optical properties under an applied voltage,[1, 2] are of much interest for practical applications in displays, smart windows, and reflectance mirrors.[3–5] For electrochromic materials, organic polymers like viologens[6] and inorganic metal oxides like tungsten oxide[7, 8] (WO_3) and nickel oxide[9, 10] (NiO) are two types of dominant materials. Among these electrochromic materials, NiO as an anodic coloring material is used to form the complementary electrochromic device with cathodic coloring material WO_3, and has been studied since 1980s owing to its high electrochromic efficiency, good cyclic durability, and low cost.[11–13]

NiO is a *p*-type semiconductor with cation vacancies, electrically compensated by electronic holes, as the primary defects which leads to the formation of Ni^{3+} states.[14] The coloring and bleaching in NiO are associated with a charge transfer between Ni^{2+} and Ni^{3+} states.[15] Therefore, careful control the proportion of Ni^{2+} and Ni^{3+} ions plays a critical role in improving the electrochromism of NiO. Magnetron sputtering technology is an effective way to adjust the O_2 concentration of sputtering atmosphere by varying the Ar/O_2 ratio,[16, 17] here the proportion of Ni^{2+} and Ni^{3+} ions in NiO_x films is sensitive to the O_2 concentration. The electrochromism of NiO_x films with $1.16 \leq x \leq 1.32$ was significantly enhanced at large values of x.[18] Charge exchange in NiO_x films was mainly due to surface processes and involved both cation and anions from the electrolyte. Further, NiO_x films were magnetron sputtered in Ar/O_2 mixing gases with the O_2 concentration varied from 4.5% to 20%.[15] NiO_x films deposited at 6% O_2 concentration displayed large transmittance modulation of 40% due to the poor crystalline structure and less proportion of Ni^{3+} ions. However, the transmittance modulation and color efficiency were relative low and the mechanism of electrochromism in NiO_x films was poorly understood. Therefore, it is essential to make further efforts to research the electrochromic properties of NiO_x films at different O_2

*Author to whom correspondence should be addressed.

concentration, improve the transmittance modulation and color efficiency, and understand the mechanism of electrochromism.

This paper reports on a detailed study of electrochromic properties in NiO_x films. The NiO_x films were deposited onto ITO-coated glass substrates by magnetron sputtering in Ar/O_2 mixing gas with different O_2 concentration. The crystalline structure, surface morphology, electrochemical and optical properties were measured and analyzed in order to investigate the mechanism of electrochromism. NiO_x film deposited at 15% O_2 concentration had the good cyclic durability. All films had the large transmittance modulation and color efficiency.

2. EXPERIMENTAL DETAILS

NiO_x films were deposited at room temperature onto ITO-coated glass substrates by DC magnetron sputtering using Ni target (99.995% purity) of 7.62 cm diameter. The substrates were 2.5×2.5 cm^2 glass plates with ITO layer having a sheet resistance of 30 Ω/Sq. The distance from substrate to Ni target was 10 cm. The chamber was evacuated to a base pressure of 5×10^{-4} Pa. A mixture of argon (99.995%) and oxygen (99.995%) was used for the sputtering atmosphere, and the sputtering power was fixed at 100 W. During deposition, the O_2 concentration (O_2/(O_2+Ar) gas-flow ratio) was varied from 8% to 20%, and the total sputtering pressure was kept constant at 0.3 Pa. Presputter was performed for 10 min to eliminate contamination from the target. The substrate was kept uniform rotation during the sputtering process in order to ensure the uniformity of NiO_x films.

The film thickness was determined by surface profilometry using a DektakXT instrument and all the NiO_x films had a thicknesses of ~250 nm. Film crystalline structure was determined by X-ray diffraction (XRD) using a APEX II DUO diffractometer with CuK α radiation at a wavelength of 0.154 nm. Structure and phase composition were obtained by comparison with the Joint Commission of Powder Diffraction Standards (JCPDS) database. The valence state of nickel was measured by X-ray photoelectron spectroscopy (XPS, ESCALAB 250, Thermofisher, UK). Surface morphology of the films was characterized by scanning electron microscope (SEM, SUPRA 55, Zeiss, Germany) and atomic force microscope (AFM, Veeco, America). Cyclic voltammetry (CV) measurement and chemical diffusion coefficient (D) for lithium ions were carried out using conventional three-electrode configuration on a CHI660E electrochemical workstation. Pt foil and Ag/AgCl electrodes were used as counter and reference electrodes respectively, and the NiO_x film was used as working electrode. The electrolyte was a 1 M $LiClO_4$-PC solution. Ionic conductivity was measured by using the Electrochemical Impedance Spectroscope (EIS). Optical transmittance measurement was recorded *in situ* during electrochemical cycling in the 330–800 nm wavelength range (Lambda950, PerkinElmer).

3. RESULTS AND DISCUSSION

Figure 1 shows the X-ray diffraction profiles of NiO_x films deposited at different O_2 concentration. XRD spectra indicated NiO_x films with cubic fcc structure (JCPDS No. 47-1049) have a polycrystalline structure with four diffraction peaks corresponding to (111), (200), (220), and (311) planes. No other peaks of impurity appeared, such as Ni_2O_3, NiOOH, or NiO_2. However, the color of as-deposited films is dark brown which implies the appearance of Ni^{3+} ions in Ni_2O_3 or NiOOH configuration.[19] Beacuse the Ni^{3+} ions act as the color centers in NiO_x films and Ni_2O_3 or NiOOH exists in amorphous state. Therefore, the XPS measurement was carried out to investigate the chemical valence state of nickel in NiO_x films. Figure 2 shows the typical XPS survey spectra of as-prepared NiO_x films. According to literature data,[20–22] the peak at binding energy 853.8 ev can be assigned to

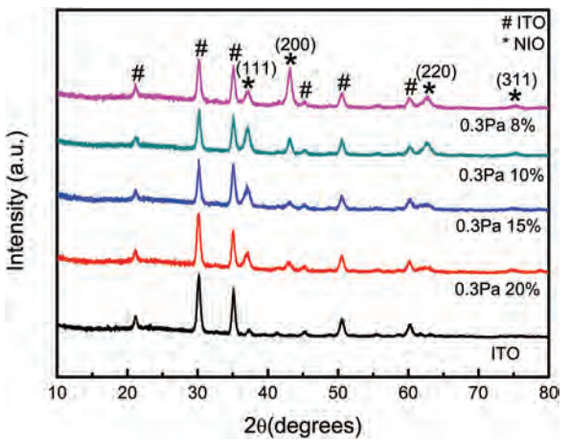

Figure 1. XRD patterns of NiO_x films deposited at different O_2 concentration.

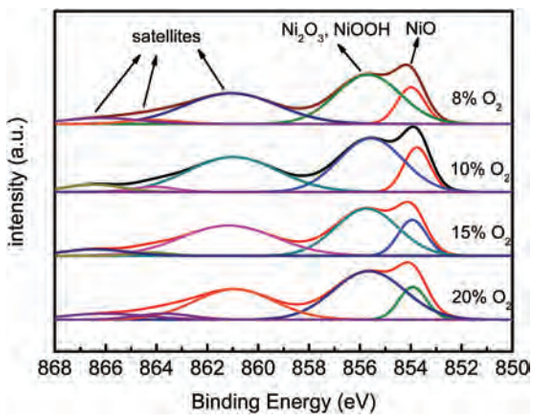

Figure 2. XPS spectra of NiO_x films deposited at different O_2 concentration.

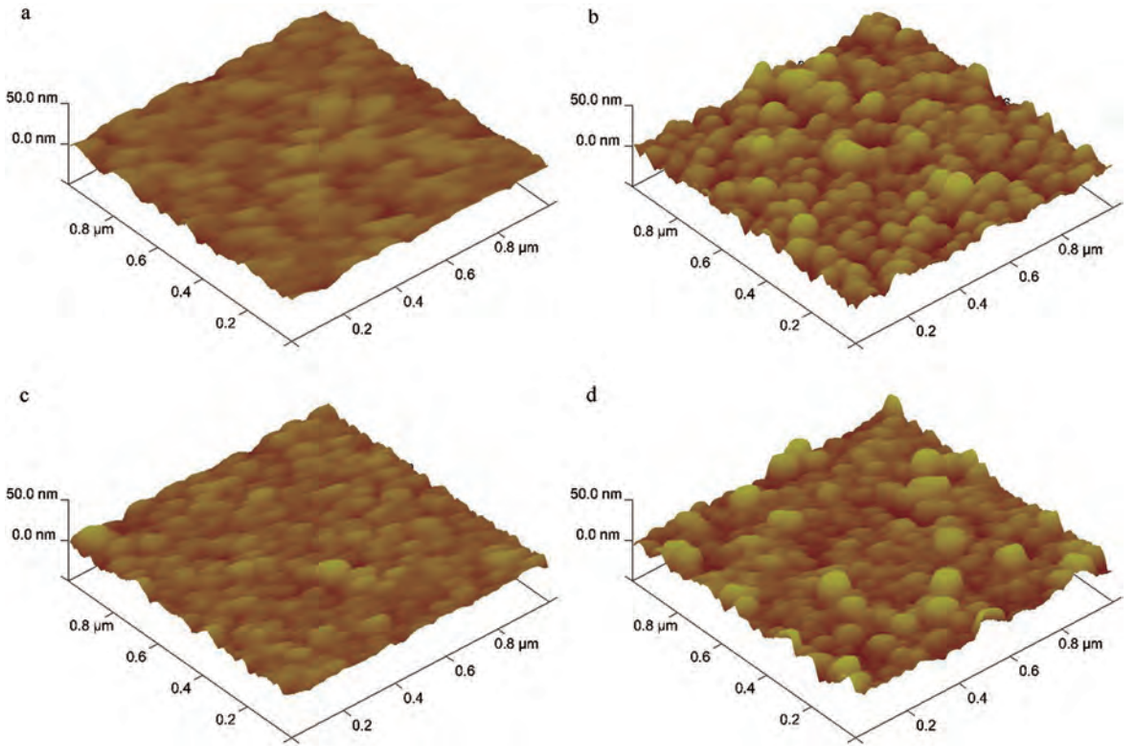

Figure 3. AFM images of NiO_x films with the O_2 concentration of (a) 8%, (b) 10%, (c) 15%, and (d) 20%.

Ni^{2+} (NiO) and 855.6 ev to Ni^{3+} (Ni_2O_3 or NiOOH). The relative peak height of (111) and (200) peaks largely depends on the O_2 concentration. NiO_x film deposited at 8% O_2 concentration has a stronger peak for the (200) growth direction than that of (111) peak. As O_2 concentration increases, the (200) peak recedes and (111) peak strengthens. Therefore, low O_2 concentration is in favor of (200) growth of NiO_x films and a sufficient amount of O_2

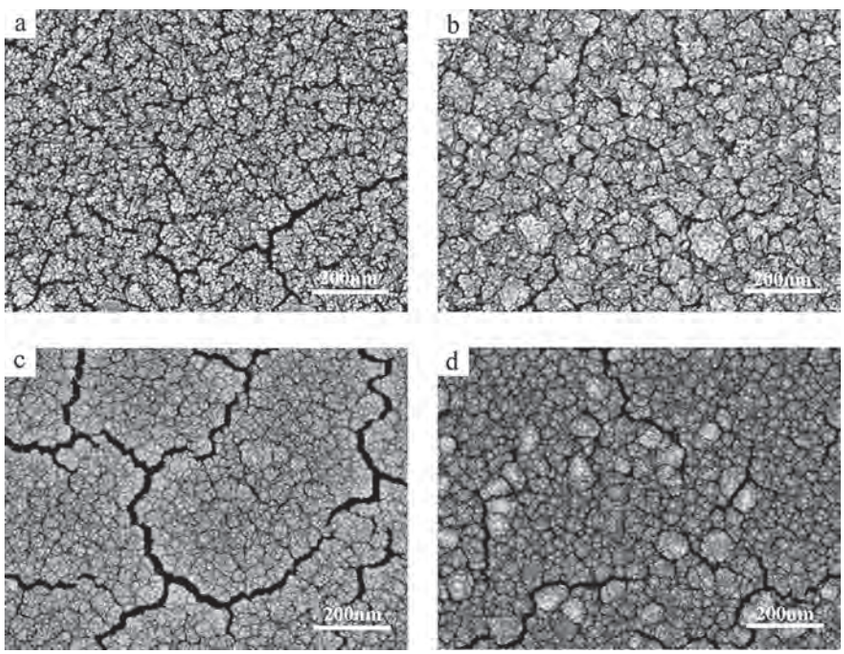

Figure 4. SEM images of NiO_x films deposited at the O_2 concentration of (a) 8%, (b) 10%, (c) 15%, and (d) 20%.

is beneficial for (111) growth, which are in agreement with the prior experimental results.[15, 18] Crystallite sizes were estimated from Scherrer's formula[23] $D = 0.89\lambda/\beta\text{Cos}\theta$ applied to the diffraction peak at 37° and were found to be 15.1 nm, 16.0 nm, 9.9 nm, and 13.1 nm for NiO_x films deposited at 8%, 10%, 15% and 20% O_2 concentration respectively. Small crystallite size was observed in NiO_x film with 15% O_2 concentration. It is predictable that NiO_x film deposited at 15% O_2 concentration has the better transmittance modulation and cyclic durability due to its poor polycrystalline structure which is generally believed to be in favor of ion transportation.[24, 25]

The AFM topography of NiO_x films are presented in Figure 3. AFM observations show clear grains and compact surface. NiO_x films deposited at 8%, 10% and 20% O_2 concentration have the large grain size, meanwhile NiO_x

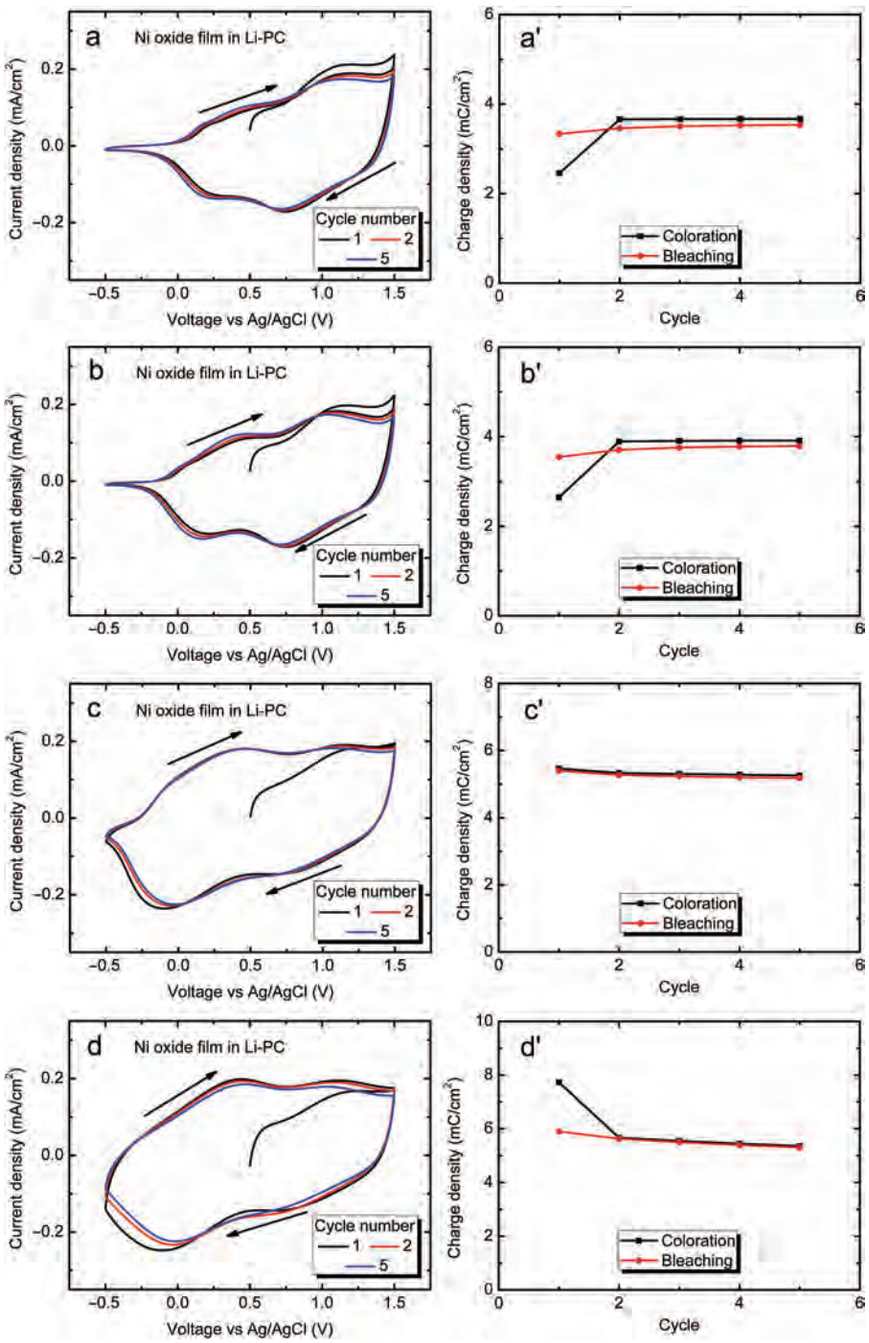

Figure 5. Cyclic voltammograms of NiO_x films with the O_2 concentration of (a) 8%, (b) 10%, (c) 15%, and (d) 20%, immersed in 1 M $LiClO_4$-PC electrolyte. The voltage sweep rate was 50 mV/s and arrows denote sweep direction. (a'–d') Charge densities obtained from CV data in (a–d).

film with 15% O_2 concentration has the small grain size. The root mean square roughness (R_{rms}) is found to be 3.84 nm, 6.46 nm, 3.63 nm, and 7.23 nm for NiO_x films deposited at 8%, 10%, 15%, and 20% O_2 concentration, respectively. Consequently, R_{rms} depends on the O_2 concentration and NiO_x film with 15% O_2 concentration has the smooth surface.

Figure 4 reports the scanning electron microscope (SEM) images of as-deposited NiO_x films. The morphology and dispersion of grain size are uniform when NiO_x film was deposited at 15% O_2 concentration, however, some remarkable cracks appear which may be attributed to the stress resulting from nickel vacancy defects or interstitial oxygen.[26] Such cracks may cause deterioration of film properties. NiO_x films with 10% and 20% O_2 concentration exhibit a rough surface and large grain size, corroborating the AFM analysis.

Electrochemical properties of NiO_x films are plotted in Figure 5 by cyclic voltammetry in a 1 M $LiClO_4$-PC electrolyte solution. Cyclic voltammetry measurement was carried out using conventional three-electrode configuration,[27,28] and performed with a linear potential sweep between −0.5 V to +1.5 V versus Ag/AgCl and a voltage sweep rate of 50 mV/s. During the cathodic potential scans from +1.5 V to −0.5 V, the current decreases firstly and then increases. Two reductive peaks appear at 0.75 V and 0 V corresponding to the maximum of current. NiO_x films experience the reduction reaction of Ni^{3+} to Ni^{2+} ions and become transparent which corresponds to the bleached state. When the voltage is swept from −0.5 V to +1.5 V, the current gradually increases and two anodic oxidative peaks corresponding to the voltages of 0.5 V and 1 V are obtained indicating the oxidation of Ni^{2+} to Ni^{3+} ions. It leads to the coloring of NiO_x films, which corresponds to the colored state. A simplified two-step scheme implying the gradual change in the optical density upon insertion/extraction of Li^+ ions in NiO_x films is represented by the following equations as suggested by Passerimi et al.[29] It refers to an initial irreversible bleaching of as-deposited NiO_x film, $NiO_x + yLi^+ + ye^- \rightarrow Li_yNiO_x$, where e^- represents electrons, followed by a reversible reaction between bleached Li_yNiO_x and colored $Li_{y-z}NiO_x$ as shown by $Li_yNiO_x \leftrightarrow Li_{y-z}NiO_x + zLi^+ + ze^-$. The cyclic voltammograms are dependent on the O_2 concentration. The area of CV loop at 8% and 10% O_2 concentration is relative small indicating the small charge exchange and the opposite trend is observed for NiO_x films deposited at 15% and 20% O_2 concentration, which are in accordance with the results of change density Q shown in Figures 5(a')–(d'). NiO_x films display almost the same charge insertion and extraction properties after the first CV cycle. Importantly, NiO_x film deposited at 15% O_2 concentration shows good cyclic durability because of its poor polycrystalline structure. Further on, cyclic voltammogram of NiO_x film with 15% O_2 concentration was performed by 1000 cycles which shows the good cyclic durability (Fig. 6).

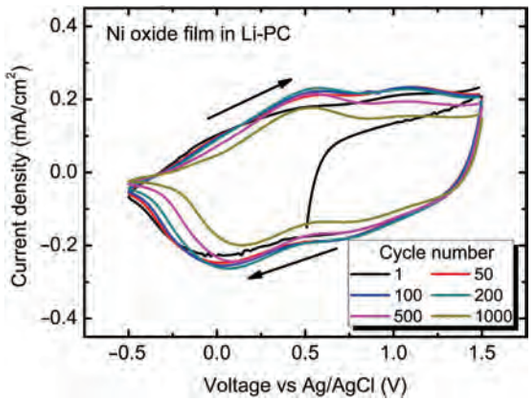

Figure 6. Cyclic voltammogram of NiO_x film deposited at 15% O_2 concentration in 1 M $LiClO_4$-PC electrolyte. The voltage sweep rate was 50 mV/s and arrows denote sweep direction.

The diffusion coefficient D of Li^+ ions is calculated by using the Randles-Sevcik equation:[14] $i_p = 2.69 \times 10^5 n^{3/2} AD^{1/2} Cv^{1/2}$, where i_p is the peak current, n is the number of electrons participating in the electrochemical reaction which is normally 1, A is the area of electrode, D is the diffusion coefficient of Li^+ ions, C is the concentration of active ions in the electrolyte solution, v is the sweep rate. The peak current is obtained from the cyclic voltammograms at the different sweep rate (not shown here). The anodic and cathodic diffusion coefficients are shown in Table I. It is clearly shown that both the anodic and cathodic diffusion coefficients of NiO_x films deposited at 15% and 20% O_2 concentration are larger than that of 8% and 10% O_2 concentration, which indicates the better cyclic voltammograms shown in Figure 5. The ionic conductivity (σ) was measured by using the Electrochemical Impedance Spectroscope (EIS) and is shown in Table I. The ionic conductivity of 4.97×10^{-6} $cm^{-2}s$, 5.95×10^{-6} $cm^{-2}s$, 6.5×10^{-6} $cm^{-2}s$, and 5.46×10^{-6} $cm^{-2}s$ are obtained for NiO_x films deposited at 8%, 10%, 15%, and 20% O_2 concentration, respectively. The largest ionic conductivity is obtained for NiO_x film with 15% O_2 concentration which has the better electrochemical activity.

Figure 7 shows the spectral optical transmittance of NiO_x films for the same films in initial state, colored state,

Table I. Diffusion coefficient D of Li^+ ions and ionic conductivity σ for NiO_x films deposited at different O_2 concentration.

O_2 concentration (%)	Diffusion coefficient (cm^2s^{-1})		σ ($cm^{-2}s$)
	D_{anodic}	$D_{cathodic}$	
8	2.71×10^{-10}	7.99×10^{-11}	4.97×10^{-6}
10	9.02×10^{-11}	5.75×10^{-12}	5.95×10^{-6}
15	3.22×10^{-10}	2.35×10^{-10}	6.50×10^{-6}
20	3.57×10^{-10}	1.66×10^{-10}	5.46×10^{-6}

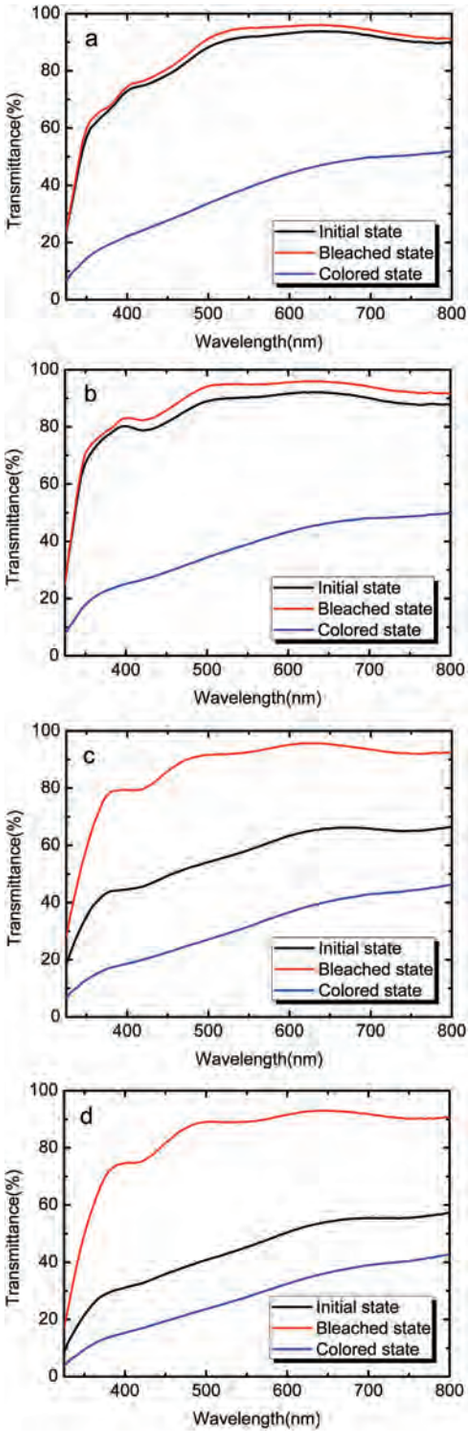

Figure 7. Spectral transmittance of NiO_x films with the O_2 concentration of (a) 8%, (b) 10%, (c) 15%, and (d) 20% in 1 M $LiClO_4$-PC electrolyte. The applied voltages of bleached state and colored state are −2 V and 2 V, respectively.

and bleached state. The transmittances of colored state and bleached state were measured by applying ±2 V in 1 M $LiClO_4$-PC electrolyte. At low O_2 concentration (8% and 10%), the transmittance of initial state films is near 90% at the wavelength of 550 nm. Moreover, the larger the O_2 concentration, the lower the transmittance of initial state films. The transmittance is 58.3% and 45.3% for NiO_x films deposited at 15% and 20% O_2 concentration, respectively. It may be attributed to a higher proportion of Ni^{3+} ions and a large amount of Ni vacancies in NiO_x films with higher O_2 concentration. These observations are in agreement with the other experimental results.[18] NiO_x films with 8% and 10% O_2 concentration have a small difference of transmittance between initial state and bleached state due to its less proportion of Ni^{3+} ions participating in the reduction reaction of Ni^{3+} to Ni^{2+} ions. On the other hand, NiO_x films at high O_2 concentration possessing high proportion of Ni^{3+} ions have the reduction reaction of Ni^{3+} to Ni^{2+} ions which results in the enhancement of transmittance from 50% to 90% and then NiO_x films became transparent. When +2 V voltage is applied to the bleached films, NiO_x films show the oxidation reaction of Ni^{2+} to Ni^{3+} ions which leads to the decrease of transmittance and NiO_x films became dark brown. The transmittance modulations are 58.2%, 55.8%, 61%, and 61.4% for NiO_x films with 8%, 10%, 15%, and 20% O_2 concentration, respectively. We can see that the transmittance modulation hardly depends on O_2 concentration. Electrochemical and optical transmittance measurements are employed to calculate the color efficiency (CE), which is defined as the difference in optical density per amount of charge exchange (ΔQ) and is given by the following equations: $CE = (\Delta OD/\Delta Q)_{\lambda=550\ nm}$ and $\Delta OD = (\log T_b/T_c)_{\lambda=550\ nm}$, where T_b and T_c are the transmittance of the films in the bleached state and colored state respectively at the wavelength of 550 nm, Δ OD is the optical density.[23] The values of optical density and color efficiency are shown in Table II. NiO_x films have the larger color efficiency of more than ∼90 cm^2C^{-1} than the other experimental results.[12, 19, 23] As expected, NiO_x film deposited at 15% O_2 concentration has the smallest color efficiency because of the cracks appeared on the surface of the film.

Figure 8 gives the coloring and bleaching response times obtained from the lifetime cycle measurement for NiO_x films. The samples were tested on a 1 M $LiClO_4$-PC electrolyte under coloring/bleaching cycles of 30 s each. Coloring and bleaching response times are defined as the time

Table II. Optical density and color efficiency of NiO_x films with different O_2 concentration.

O_2 concentration (%)	Transmittance (T_b) at 550 nm	Transmittance (T_c) at 550 nm	ΔT (%)	Optical density (Δ OD)	Color efficiency (cm^2C^{-1})
8	95.0	39.3	55.7	0.38	104
10	94.8	39.0	55.8	0.39	100
15	92.6	31.6	61.0	0.47	89
20	89.2	27.8	61.4	0.51	93

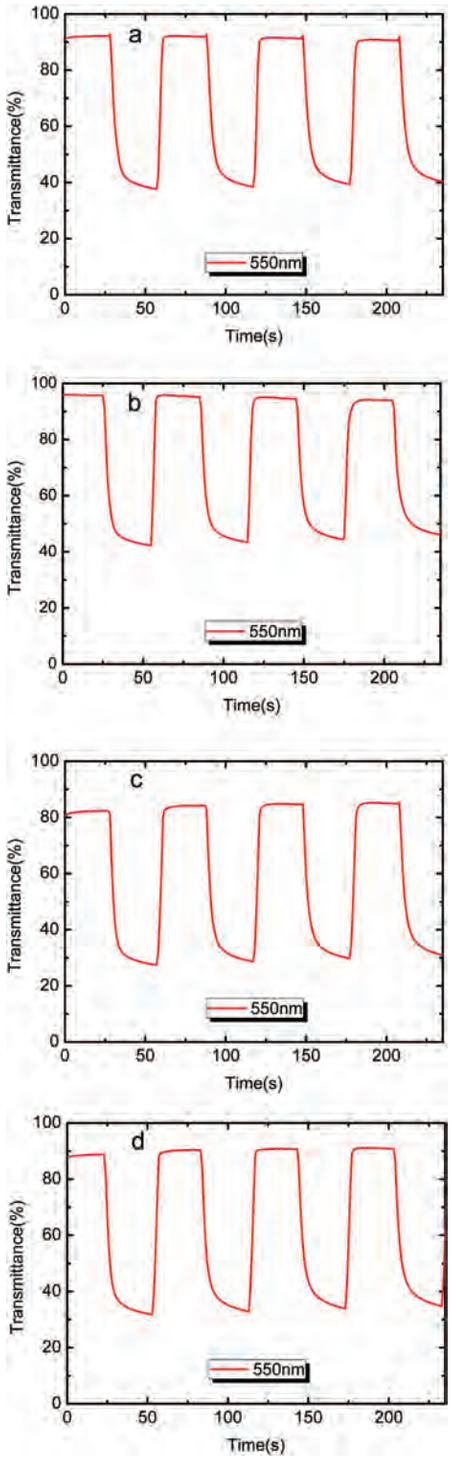

Figure 8. Lifetime cycle measurements of NiO_x films with the O_2 concentration of (a) 8%, (b) 10%, (c) 15%, and (d) 20%.

required for 90% changes in the entire transmittance modulation. The coloring response times are 9 s, 9 s, 9 s, and 11 s, while the bleaching response times are 4 s, 3 s, 4 s, and 4 s for NiO_x films deposited at 8%, 10%, 15%, and 20% O_2 concentration, respectively. It is obviously that the coloring/bleaching response time is independent on the O_2 concentration because NiO_x films deposited at different O_2 concentration have the similar compact structure. Moreover, the bleaching process is faster than the coloring process. Because NiO_x films have the low conductive NiO and highly conductive Ni_2O_3 or NiOOH. The intercalation of Li^+ ions during the bleaching process is easier than the deintercalation during the coloring process.[30] Therefore, the transition from the Ni_2O_3 or NiOOH to NiO is faster than that from the NiO to Ni_2O_3 or NiOOH.

4. CONCLUSIONS

The effect of O_2 concentration on the structure, morphology, electrochemical properties, and optical transmittance properties of NiO_x films was investigated by DC magnetron sputtering technology. X-ray diffraction analysis shows low O_2 concentration is beneficial for preferred (200) growth and high O_2 concentration is in favor of (111) growth of NiO_x films. The morphology measurements indicate NiO_x film deposited at 15% O_2 concentration has the small grain size and smooth surface. The cyclic voltammogram and charge density of NiO_x films largely depend on the O_2 concentration, whereas the transmittance modulation and coloring/bleaching response time are almost independent on the O_2 concentration. The good cyclic durability, large transmittance modulation, high color efficiency, and fast coloring/bleaching response time make NiO_x films suitable for application in electrochromic window as an anodic coloring material.

Acknowledgments: This project is supported by the Priority Academic Program Development of Jiangsu Higher Education Institutions, the research fund of Jiangsu Province Cultivation base for State Key Laboratory of Photovoltaic Science and Technology, Major Projects of Natural Science Research in Jiangsu Province 15KJA43002 and 16KJD430006, and China Postdoctoral Science Foundation 2017M611719.

References and Notes

1. B. D. R. Rosseinsky and R. J. Mortimer, *Adv. Mater.* 13, 783 (**2001**).
2. V. K. Thakur, G. Q. Ding, J. Ma, P. S. Lee, and X. H. Lu, *Adv. Mater.* 24, 4071 (**2012**).
3. C. G. Granqvist, *Sol. Energy Mater. Sol. Cells* 60, 201 (**2000**).
4. C. G. Granqvist, Handbook of Inorganic Electrochromic Materials, Elsevier Science B. B. V., Amsterdam (**1995**).
5. C. G. Granqvist, Handbook of Electrocemistry, CRC Press, Boca Raton (**1997**), p. 587.
6. R. Vergaz, D. Barrios, J. Sanchez-Pana, C. Pozo-Gonzalo, and M. Salsamendi, *Sol. Energy Mater. Sol. Cells* 93, 2125 (**2009**).
7. G. A. Niklasson and C. G. Granqvist, *J. Mater. Chem.* 17, 127 (**2007**).
8. V. R. Bucha, A. K. Chawla, and S. K. Rawal, *Materials Today: Proceedings* 3, 1429 (**2016**).
9. Y. Ren, W. K. Chim, L. Guo, H. Tanoto, J. S. Pan, and S. Y. Chiam, *Sol. Energy Mater. Sol. Cells* 116, 83 (**2013**).

10. K. K. Purushothaman and G. Muralidhran, *Sol. Energy Mater. Sol. Cells* 93, 1195 **(2009)**.
11. S. H. Park, J. W. Lim, S. J. Yoo, I. Y. Cha, and Y. E. Sung, *Sol. Energy Mater. Sol. Cells* 99, 31 **(2012)**.
12. S. Pereira, A. Goncalves, N. Correia, J. Pinto, L. Pereira, R. Martins, and E. Fortunato, *Sol. Energy Mater. Sol. Cells* 120, 109 **(2014)**.
13. H. J. Ahn, H. S. Shim, Y. S. Kim, C. Y. Kim, and T. Y. Seong, *Electrochem. Commun.* 7, 567 **(2015)**.
14. K. S. Usha, R. Sivakumar, C. Sanjeeviraja, V. Sathe, V. Ganesan, and T. Y. Wang, *RSC Adv.* 6, 79668 **(2016)**.
15. X. W. Song, G. B. Dong, F. Y. Gao, Y. Xiao, Q. R. Liu, and X. G. Diao, *Vacuum* 111, 48 **(2015)**.
16. S. Yamada, T. Yoshioka, M. Miyashita, K. Urabe, and M. Kitao, *J. Appl. Phys.* 63, 2116 **(1988)**.
17. L. Ottaviano, A. Pennisi, and F. Simone, *Surf. Interface Anal.* 36, 1335 **(2004)**.
18. R. T. Wen, C. G. Granqvist, and G. A. Niklasson, *Adv. Funct. Mater.* 25, 3359 **(2015)**.
19. D. M. Dong, W. W. Wang, G. B. Dong, Y. L. Zhou, Z. H. Wu, M. Wang, F. M. Liu, and X. G. Diao, *Appl. Surf. Sci.* 357, 799 **(2015)**.
20. M. C. Biesinger, B. P. Payne, L. W. M. Lau, A. Gerson, and R. S. C. Smart, *Surf. Interface Anal.* 41, 324 **(2009)**.
21. S. Oswald and W. Bruckner, *Surf. Interface Anal.* 36, 17 **(2004)**.
22. C. C. Wu and C. F. Yang, *Nanoscale Res. Lett.* 8, 33 **(2013)**.
23. R. T. Wen, G. A. Niklasson, and C. G. Granqvist, *Thin Solid Films* 565, 128 **(2014)**.
24. X. G. Wang, Y. S. Jang, and N. H. Yang, *Sol. Energy Mater. Sol. Cells* 63, 197 **(2000)**.
25. A. Georg, W. Graf, and R. Neumann, *Solid State Ionics* 127, 319 **(2000)**.
26. S. Seo, M. J. Lee, D. H. Seo, E. J. Jeoung, D. S. Suh, Y. S. Joung, I. K. Yoo, I. R. Hwang, S. H. Kim, I. S. Byun, J. S. Kim, J. S. Choi, and B. H. Park, *Appl. Phys. Lett.* 85, 5655 **(2004)**.
27. A. H. Khan, S. Ghosh, B. Pradhan, A. Dalui, L. K. Shrestha, S. Acharya, and K. Ariga, *Bull. Chem. Soc. Jpn.* 90, 627 **(2017)**.
28. Y. Wang, C. C. Mayorga-Martinez, and M. Pumera, *Bull. Chem. Soc. Jpn.* 90, 847 **(2017)**.
29. S. Passerini, B. Scrosati, and A. Gorenstein, *J. Electrochem. Soc.* 137, 3297 **(1990)**.
30. K. S. Ahn, Y. C. Nah, and Y. E. Sung, *Appl. Surf. Sci.* 199, 259 **(2002)**.

Received: 21 July 2017. Accepted: 3 September 2017.